THE JOURNAL OF COMPARATIVE NEUROLOGY 428:278–293 (2000)

Organization of Callosal Linkages in Visual Area V2 of Macaque Monkey

PAUL L. ABEL, BRENDAN J. O'BRIEN, AND JAIME F. OLAVARRIA*
Department of Psychology, University of Washington, Seattle, Washington 98195-1525

ABSTRACT

In visual area V2 of the macaque monkey callosal cells accumulate in finger-like bands that extend 7–8 mm from the V1/V2 border, or approximately half the width of area V2. The present study investigated whether or not callosal connections in area V2 link loci that are located at the same distance from the V1/V2 border in both hemispheres. We analyzed the patterns of retrograde labeling in V2 resulting from restricted injections of fluorescent tracers placed at different distances from the V1/V2 border in contralateral area V2. The results show that varying the distance of V2 tracer injections from the V1/V2 border led to a corresponding variation in the location of labeled callosal cells in contralateral V2. Injections into V2 placed on or close to the V1 border produced labeled cells that accumulated on or close to the V1 border in contralateral V2, whereas injections into V2 placed away from the V1 border produced labeled cells that accumulated mainly away from the V1 border. These results provide evidence that callosal fibers in V2 preferentially link loci that are located at similar distances from the V1/V2 border in both hemispheres. Relating this connectivity pattern to the topographic map of V2 suggests that callosal fibers link topographically mirror-symmetrical regions of V2, i.e., callosal fibers near the V1/V2 border interconnect areas representing visual fields on, or close to, the vertical meridian, whereas callosal connections from regions away from the V1/V2 border interconnect visuotopically mismatched visual fields that extend onto opposite hemifields. J. Comp. Neurol. 428: 278–293, 2000.

Indexing terms: interhemispheric commissure; corpus callosum; extrastriate cortex; visual topography

Numerous studies on the interhemispheric connections through the corpus callosum have led to the notion that, in visual cortex, these connections are restricted to borders of visual areas where the vertical meridian of the visual field is represented (Mettler, 1935; Myers, 1962, 1965; Ebner and Myers, 1965; Hubel and Wiesel, 1967; Cragg, 1969; Zeki, 1969, 1970). However, more recent studies have shown that in many visual areas the distribution of callosal connections is more widespread, extending into regions that represent fields located away from the vertical meridian (Segraves and Rosenquist, 1982a,b; Van Essen et al., 1982; Olavarria and Van Sluyters, 1983; Cusick et al., 1984, 1985; Cusick and Kaas, 1986; Maunsell and Van Essen, 1987). These observations raise the issue of the point-to-point organization of callosal linkages and its relationship to the underlying topography of visual cortex. For instance, do callosal fibers link loci that represent the same visual field coordinates, or do they instead link regions in both hemispheres that represent parts of the visual field that are mirror-symmetrical relative to the vertical meridian? Understanding the organization of callosal linkages and its relationship to the underlying visual topography may be crucial for formulating theories about the function of the callosal pathway. This knowledge may also yield clues about the mechanisms that guide the development of interhemispheric connections.

We were interested in comparing the rules of callosal connectivity in V2 of macaques with those that have been described for the callosal zone at the lateral border of striate cortex in rats and cats. In these species, callosal fibers link regions that are located at different distances

Grant sponsor: National Institutes of Health; Grant numbers: T32 EY07031, EY09343.

Dr. Abel's current address is: Intel Corporation, New Business Group, Connected Products Division JF2-11, 2111 N.E. 25th Avenue, Hillsboro, OR 97124-5961.

Dr. O'Brien's current address is: Neuroanatomie, Max Planck Institut für Hirnforchung, Deutschordenstrasse 46 D-60528, Frankfurt, Germany.

*Correspondence to: Jaime F. Olavarria, Department of Psychology, University of Washington, Box 351525, Seattle, WA 98195-1525.
E-mail: jaime@u.washington.edu

Received 18 May 1999; Revised 22 August 2000; Accepted 28 August 2000

from the V1 border but that represent the same visual field coordinates. For instance, tracer injection at the 17/18 border (in regions representing ipsilateral visual fields) produce callosal labeling in regions located away from the 17/18 border, whereas injections away from the 17/18 border produce labeling at the contralateral 17/18 border (Lewis and Olavarria, 1995; Olavarria, 1996). Studying the fine connectivity of callosal connections in macaque V1 is difficult, because, unlike the rat and cat, callosal connections are sparse and largely restricted to a very narrow zone at the V1 border (Myers, 1962; Lund et al., 1975; Van Essen and Zeki, 1978; Kennedy et al., 1986; Olavarria and Abel, 1996). On the other hand, area V2 in macaques exhibits an extensive and robust pattern of callosal connections (Zeki, 1970; Van Essen and Zeki, 1978; Van Essen et al., 1982; Kennedy et al., 1986; Olavarria and Abel, 1996) that lends itself to studies of the topographic organization of this pathway. Callosal cells in macaque area V2 accumulate in finger-like bands that protrude 7–8 mm into this area (Olavarria and Abel, 1996). We examined the organization of callosal linkages in V2 by placing restricted injections of fluorescent tracers into V2 at different distances from the V1 border and later analyzing the resulting distribution of retrogradely labeled cells in contralateral V2. In contrast to previous findings in striate cortex of the rat and cat (Lewis and Olavarria, 1995; Olavarria, 1996), in macaque V2, we found that both the injection sites and the resulting fields of callosal labeling were located at similar distances from the V1/V2 border. These results suggest that callosal fibers in V2 interlink cortical sites representing visual fields located on either side of the vertical meridian of the visual field. Some of these results have been presented previously as an abstract (Abel et al., 1995).

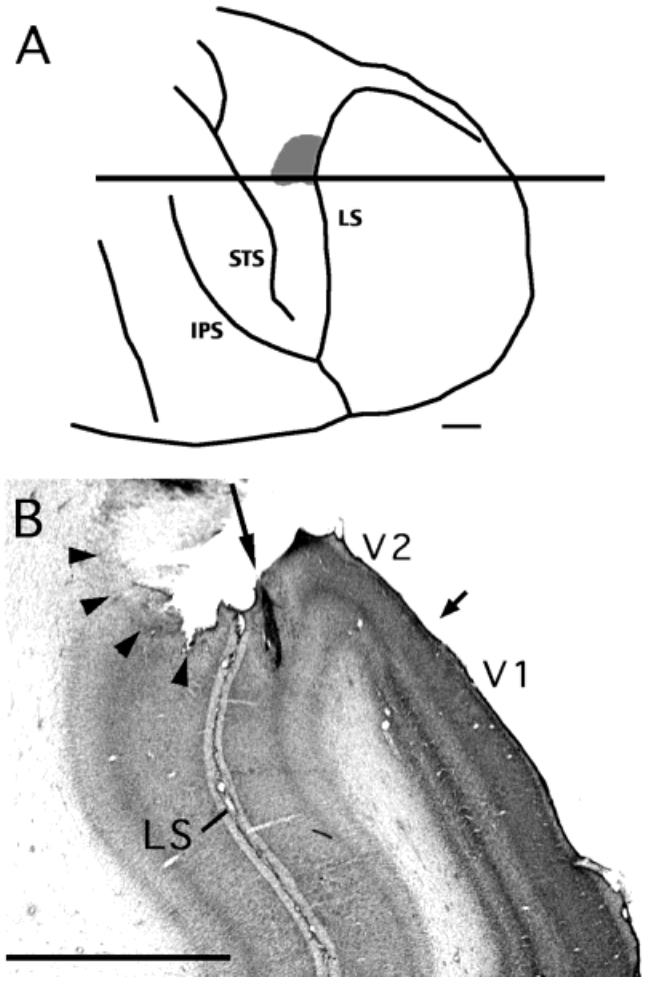

Fig. 1. **A:** Dorsal view of posterior half of right hemisphere in monkey mf-13 illustrating the procedure used for delivering tracer injections into V2. Posterior is to the right, medial is down. The gray area indicates the region of the prelunate gyrus that was aspirated to inject tracers into V2 under visual guidance. The black line indicates the location from where the parasagittal section shown in B was taken. **B:** Nissl-stained parasagittal section taken from the region indicated by the black line in A. Posterior is to the right. Arrowheads indicate the lesion in the prelunate gyrus. The long arrow indicates an injection of Nuclear Yellow into V2 placed at approximately 2.3 mm from the V1/V2 border (indicated by the short arrow). Data obtained from this animal are shown in Figure 8. LS, lunate sulcus; STS, superior temporal sulcus; IPS, intraparietal sulcus. Scale bar = 3.0 mm in B (applies to A,B).

MATERIALS AND METHODS

The present study presents data from five adult monkeys (four *Macaca fascicularis*, one *Macaca nemestrina)*, each weighing 3–6 kg. Surgery was performed aseptically under general anesthesia induced with ketamine (10 mg/kg i.m.) and maintained with halothane (1.5–3.0% in oxygen). A craniotomy and durotomy were made over the lunate, intraparietal, and superior temporal sulci in one hemisphere. A portion of the prelunate gyrus was then removed by subpial aspiration to visualize regions of V2 that are normally buried in the lunate sulcus (Fig. 1).

Restricted injections of the fluorescent tracers bisbenzimide (BB, 10% in dH_2O; Sigma) or Nuclear Yellow (NY, 5% in dH_2O; Sigma) were made into regions of area V2 that were either on the dorsal surface of the operculum, near or on the V1/V2 border, or on the posterior bank of the lunate sulcus (see Fig. 1B). Tracers were pressure-injected through glass micropipettes with 50–100 μm internal tip diameter. Each tracer was administered either in a single injection (e.g., Fig. 1B) or in multiple injections placed at the same distance from the V1/V2 border. The volume of each injection was approximately 0.2 μl, and the total volume of each tracer injected did not exceed 1.0 μl.

After a 3- to 4-day survival period, animals were deeply anesthetized with pentobarbital sodium (0.40 mg/kg i.v.) and perfused transcardially with 0.9% saline followed by a fixative solution containing 2% paraformaldehyde and 0.25% glutaraldehyde in 0.1 M phosphate buffer (pH 7.4). All surgical procedures were performed in accordance with NIH guidelines (NIH publication 85-23) and according to protocols approved by the U.W. Animal Care Committee (IACUC).

Histochemical processing

In three animals, the hemispheres were physically unfolded and flattened according to procedures described previously (Olavarria and Van Sluyters, 1985). In the other two animals, the hemispheres were analyzed in parasagittal sections. In all animals, brainstems were separated and analyzed in transverse sections. The unfolded and flattened tissue was left overnight between glass

slides at 4°C in 0.1 M phosphate buffer. The glass slides were removed, and the tissue was further fixed in a solution with 20% sucrose for approximately 30 minutes. The tissue was transferred to a solution of 20% sucrose in 0.1 M phosphate buffer at 4°C until it sank. The hemispheres to be sectioned parasagittally and all brainstems were left in the fixative solution with 20% sucrose at 4°C until they sank. All tissue blocks were sectioned at 40–50 μm on a freezing microtome.

Sections from the unfolded and flattened tissue were mounted onto unsubbed glass slides, air-dried, and immediately analyzed for labeled cells/injection sites under fluorescent microscopy. These sections were later removed from the slides and processed for cytochrome oxidase (CO; Wong-Riley, 1979) to reveal the location of the V1/V2 border (see Fig. 6C) or were processed for Cat-301 immunohistochemistry to aid in the identification of CO-stripes (Hendry et al., 1988; DeYoe et al., 1990; Abel et al., 1997; Olavarria and Van Essen, 1997; the Cat-301 monoclonal antibody was kindly provided by Susan Hockfield). From each block, a few sections that had not been analyzed for fluorescent labeling were also processed for CO, because we noted that CO staining was weaker in those restricted areas that were examined under fluorescent microscopy for a long time (see Fig. 6C). Every fourth parasagittal section (200-μm interval) was mounted onto subbed slides and analyzed for cortical injection sites and retrogradely labeled cells. The same sampling interval was used to analyze retrograde labeling in the thalamus in transverse sections. Parasagittal and transverse sections were then stained for Nissl substance to reveal cortical (Fig. 1B) or thalamic architecture.

Data analysis

Histologic sections were analyzed by using a microscope equipped with a motorized stage controlled by computer running the graphic system Neurolucida (MicroBrightField). The size of the V2 injections was estimated by plotting the boundaries of both the central core of intense fluorescence and the surrounding halo of diffuse fluorescence (see Figs. 5A, 6A). The distributions of labeled cells in ipsilateral V1 and thalamus were also analyzed. In some cases, the high intensity of the halo of fluorescence around the injection sites made it difficult to plot all retrogradely labeled cells in ipsilateral V1 after injections close to the V1/V2 border. In the regions of the injections, the pipette tracks and the white matter were carefully inspected to determine whether the tracers had infiltrated the underlying white matter. In one animal (case mf-09), the injections of BB were large and encroached into white matter. These injections resulted in large clusters of BB-labeled cells in several regions of the pulvinar and diffuse patterns of labeled cells in the lateral geniculate nucleus (LGN). In the contralateral hemisphere, these injections of BB labeled the entire callosal pattern for a portion of dorsal V2 (see Fig. 2; Olavarria and Abel, 1996). All other injections in this report were judged to be confined to gray matter.

Reconstructions of the distribution of labeled callosal cells in the unfolded and flattened tissue (Fig. 6B) were prepared by carefully superimposing drawings of all tangential sections containing labeled cells. After these sections were stained for CO, a line representing the V1/V2 border (Fig. 6C) was added to the drawing for each section. Alignment of the drawings was facilitated by using landmarks such as blood vessels (Fig. 6B), tissue contours, and the V1/V2 border. Figure 6C correlates the pattern of callosal labeling in V2 with the underlying pattern of CO staining in the same animal. This figure was prepared by using Photoshop 3.0 (Adobe Systems) to superimpose the reconstructed pattern of labeled callosal cells to a digitized image of the pattern of CO staining.

Quantitative analysis

The V1/V2 border, identified in CO-stained (Fig. 6C) and/or Nissl-stained (Fig. 1B) sections, was plotted onto drawings of each section. In parasagittal sections, starting at the V1/V2 border, 200-μm-wide strips were marked from the bottom of layer 4 to the cortical surface. In tangential sections, area V2 was divided into 200-μm-wide strips oriented parallel to the V1/V2 border. Labeled callosal cells within each strip were counted, and the numbers in the corresponding strips of neighboring tissue sections were summed. We also analyzed data from large tracer deposits to derive a profile of the maximum labeling density at each point across the width of V2. By using this information, the labeling densities measured at each distance from the V1/V2 border after restricted injections were expressed as a percentage of the maximum labeling density at each point. This transformation eliminated the gradual decrease of callosal cell density with increasing distance from the V1/V2 border as a confounding factor in the analysis of the organization of callosal linkages in V2 (see below).

RESULTS

In the hemisphere contralateral to the V2 injection sites, most labeled callosal cells were found in layer 3 of area V2. Relatively few callosal cells were found in V1, and most of them were located in a narrow band close to the V1/V2 border (Fig. 2A). In addition, callosal cells were found in the ventral bank of the lunate sulcus, in the annectant gyrus, posterior portions of the prelunate gyrus, and in an area extending down the posterior bank of the superior temporal sulcus. These observations are in agreement with previous studies of callosal connections in the macaque monkey (Lund et al., 1975; Van Essen et al., 1982; Kennedy et al., 1986; Olavarria and Abel, 1996).

Overall pattern of callosal connections in V2

Figure 2 shows the overall pattern of callosal connections revealed with large injections of BB in animal mf-09 of the present study. This case confirmed our previous report (Olavarria and Abel, 1996) that in the macaque callosal cells accumulate at the V1/V2 border and in finger-like bands that extend into V2. The profile of callosal cell density across the width of V2 for this case is shown in Figure 3A. This profile was constructed by counting cells in 200-μm-wide strips oriented parallel to the V1/V2 border (see Materials and Methods section). By using the same procedures, a second profile of callosal cell density across the width of V2 was prepared for one case in which the global callosal pattern was revealed by implanting pieces of polyacrylamide gel impregnated with horseradish peroxidase (HRP) into the cut corpus callosum. The overall pattern of callosal connections in V2 of this case was shown in a previous study (case 428, Fig. 3A,B in Olavarria and Abel, 1996). Both profiles are shown superimposed in Figure 3B, together with the

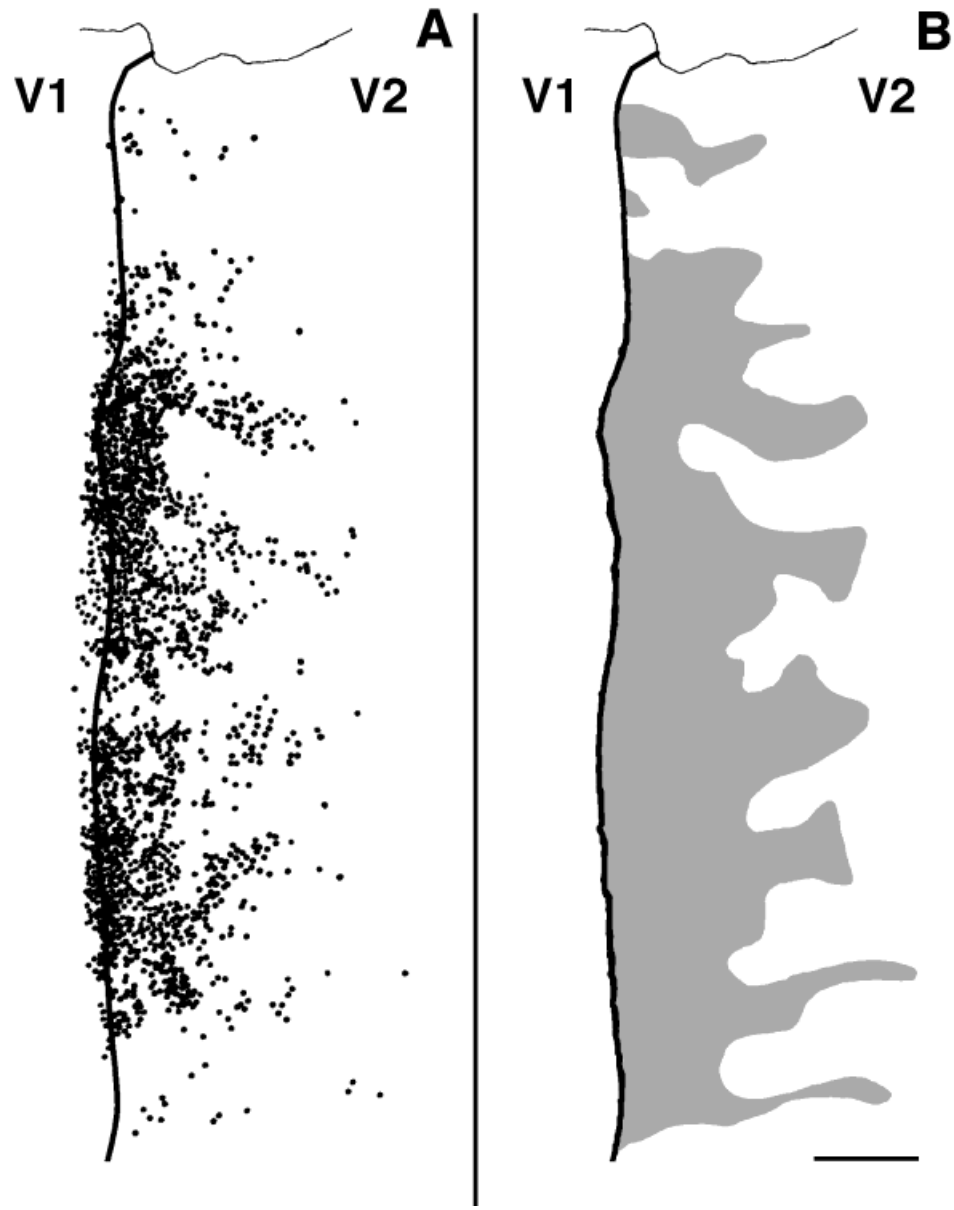

Fig. 2. **A:** Distribution of bisbenzimide-labeled callosal cells (black dots) in dorsal V2 reconstructed from tangential sections through the right hemisphere of animal mf-09. Medial is up. **B:** The shaded area indicates the envelope of the distribution of labeled cells in A. This envelope was drawn by connecting labeled cells in a way so as to preserve the finger-like appearance of callosal labeling in V2 (see also Olavarria and Abel, 1996). This shaded area is also shown in Figure 4B, together with additional data from the same animal. In A and B, the location of the line indicating the V1/V2 border was determined in cytochrome oxidase-stained sections. A graph of the density distribution across V2 of the labeling in A is shown in Figure 3A. Scale bar = 2.0 mm in B (applies to A,B).

best-fit curve drawn from both sets of data. Figure 3B shows that there is an exponential decrease in the distribution of cells across the width of V2. This decrease in cell density is due in part to the fact that callosal cells are distributed into a largely continuous band at the V1 border, whereas further into V2, the distribution breaks into bands that become progressively narrower as they extend further into V2 (see Fig. 2, and Olavarria and Abel, 1996).

Figure 3C shows hypothetical results from injections of two tracers (X and Y), which produced two discrete fields of retrogradely labeled fields located at different distances from the V1/V2 border in contralateral V2. Because of the exponential decrease in the density distribution of callosal cells across V2 (segmented curve in Fig. 3C), the maximum density that can be expected for the field located the farthest away from the V1/V2 border (Y-labeled cells) is significantly smaller than the maximum density that can be expected for the field close to the V1/V2 border (X-labeled cells). This means that a field containing a small number of labeled cells located away from the V1/V2 border is actually stronger than a field containing the same number of labeled cells at a location closer to the V1/V2

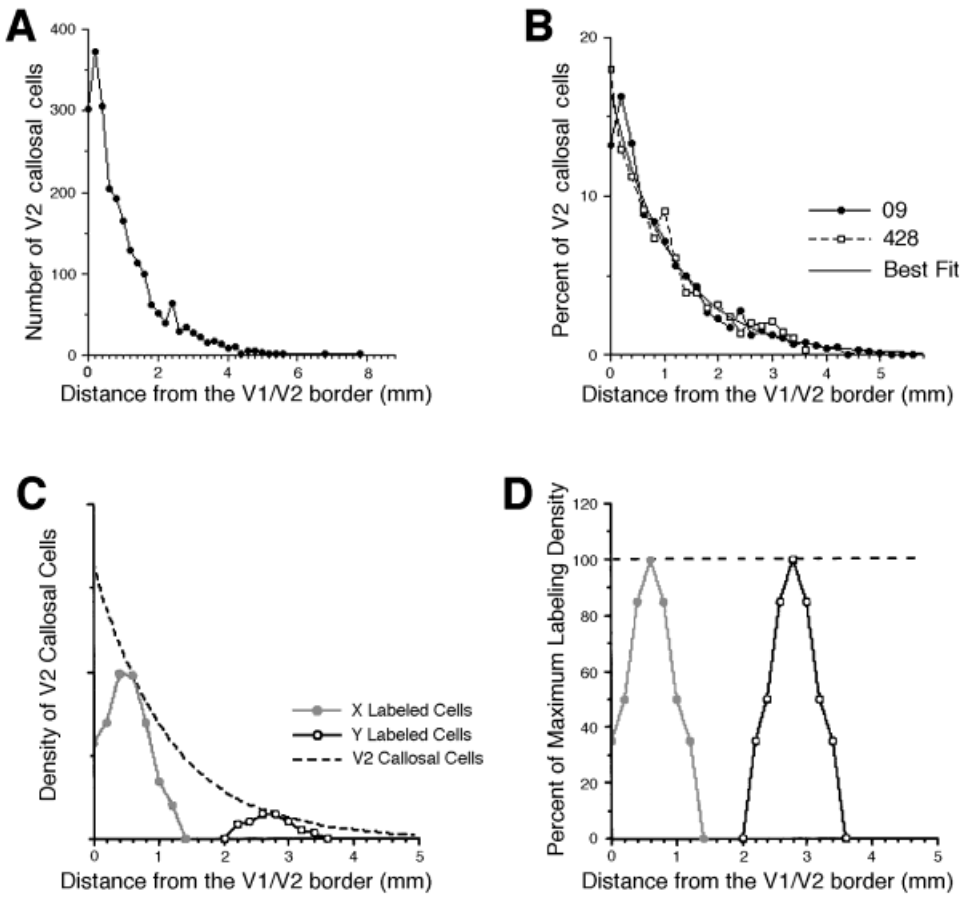

Fig. 3. **A:** Profile of labeled callosal cell density across the width of V2 for the bisbenzimide labeling shown in Figure 2A (case mf-09). This profile was constructed by counting cells in strips parallel to the V1/V2 border (see Materials and Methods section). **B:** The profile in A is shown superimposed to a graph prepared for the presented study from an animal that was studied with horseradish peroxidase and whose global pattern of V2 callosal connections was illustrated in a previous study (case 428, in Fig. 3A,B in Olavarria and Abel, 1996). Also shown is the best-fit curve calculated from both data sets. The best-fit curve shows that there is an exponential decrease in the overall distribution of cells across the width of V2. **C:** Hypothetical results from V2 injections of two tracers (X and Y) that produced discrete fields of retrogradely labeled fields located at different distances from the V1/V2 border in contralateral V2. The segmented curve represents the best-fit curve in B. This graph shows that, for injections of similar sizes, the labeling density is significantly smaller in the labeled field located the farthest from the V1/V2 border. **D:** Normalized representation of the data in C. The density of callosal labeling at each distance from the V1/V2 border is expressed as a percentage of the maximum density at each point based on the overall density distribution indicated by the segmented curve in C.

border. To compensate for the decrease in callosal cell density across the width of V2, we expressed the density of labeled cells as the percentage of the maximum labeling density at that location based on the overall density distribution shown in Figure 3B. The results obtained after normalizing the hypothetical data in Figure 3C are shown in Figure 3D. Because the distributions of X- and Y-labeled cells reach the exponential curve of maximum labeling density (Fig. 3C), these distributions reach the 100% line in Figure 3D. In all subsequent figures, the normalized distributions of labeled callosal cells are illustrated along with the reconstructions of the labeling patterns in the tangential plane.

Organization of callosal linkages in V2

The results show that varying the distance of V2 tracer injections from the V1/V2 border led to a corresponding variation in the location of labeled callosal cells in contralateral V2. Restricted tracer injections that were close to the V1/V2 border produced labeled fields close to the contralateral V1/V2 border, whereas injections placed away from the V1/V2 border produced labeled fields located preferentially away from the V1/V2 border. These results will be illustrated with data from tracer injections placed at different distances from the V1/V2 border in different animals, and from cases in which injections at different distances from the V1/V2 border were made in the same animal.

The animal that received large injections of BB to reveal the entire pattern of callosal connections for a region of V2 (case mf-09, Fig. 2) also received two small injections of NY in V2 placed away from the V1/V2 border. The centers of the NY injections were located approximately 3.5 mm from the V1 border. No NY-labeled cells were found in the LGN. The reconstruction of the NY injection sites is illustrated in Figure 4A. Because the injections were not made

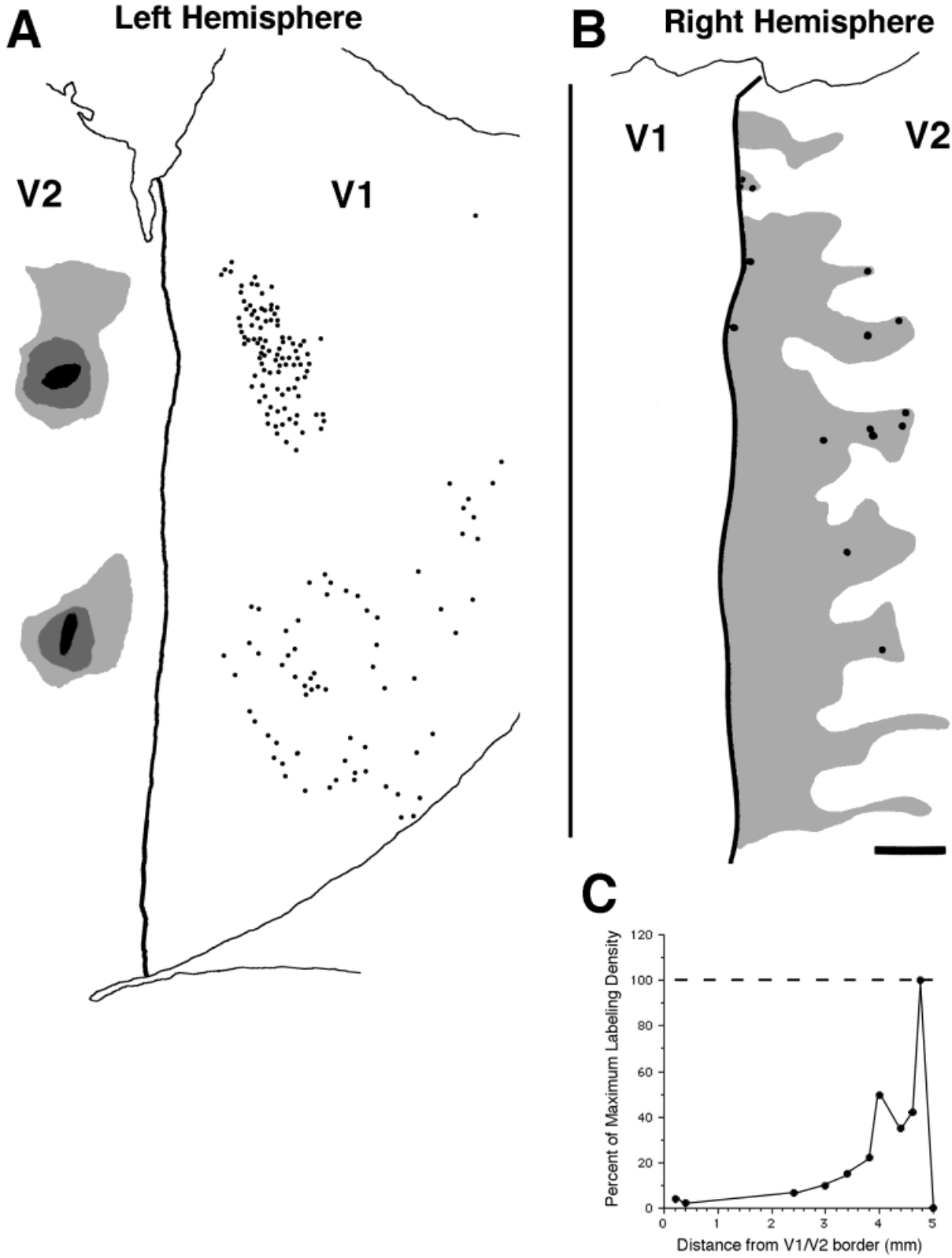

Fig. 4. **A:** Reconstruction of Nuclear Yellow (NY) injection sites in dorsal V2 and of retrogradely labeled fields in ipsilateral V1 (black dots) from tangential sections through the left hemisphere of animal mf-09. Medial is up. At the injection sites, black areas represent the injection cores, whereas the stippled surrounds represent areas of tracer diffusion. The line at the bottom of figure represents a cut through the middle of the operculum. **B:** Distribution of NY-labeled callosal cells (black dots) in dorsal V2 reconstructed from tangential sections through the right hemisphere. The shaded area (taken from Fig. 2B) represents the overall distribution of callosal cells labeled after two large injections of bisbenzimide in the left hemisphere of the same animal. In A and B, the location of the line indicating the V1/V2 border was determined in cytochrome oxidase-stained sections. **C:** Normalized distribution of NY-labeled callosal cells across the width of V2. Scale bar = 2.0 mm in B (applies to A,B).

orthogonal to the cortical surface, the pipette tracts shifted slightly across sections, leading to the oval-shaped injection cores (represented in black). In ipsilateral V1, each injection produced a field of labeled cells that roughly mirrored the location of the injection site with respect to the V1/V2 border (see black dots in Fig. 4A). The halos from the large BB injections administered to this animal (not shown) may have obscured some NY-labeled cells close to the V1 border. The field of labeled cells in V1 for the most lateral injection (bottom of Fig. 4A) was somewhat less dense than the more medial field, but it occupied a larger area. The distribution of the labeled cells within V1 agrees with previous studies that have shown a topographic organization in the pattern of V1-V2 projections (Zeki, 1969; Rockland and Pandya, 1979; Weller and Kaas, 1983; Perkel et al., 1986; Stepniewska and Kaas, 1996; Gattass et al., 1997).

The injections of NY in animal mf-09 produced a small number of labeled cells in opposite V2 (black dots in Fig. 4B). Figure 4B also shows the profile (in gray) of the overall pattern of callosal labeling obtained in the same animal with large injections of BB (see Fig. 2). Figure 4B shows that most NY-labeled cells (n = 10) were located away from the V1/V2 border, near the end of the callosal fingers revealed with BB; four cells were found near the V1/V2 border. For the reasons discussed above, the NY labeling close to the V1/V2 border represents very weak labeling at that location, whereas the labeling away from the V1/V2 border represents stronger labeling. This relationship is illustrated in the diagram of Figure 4C, which shows the normalized density distribution of NY-labeled cells. As depicted in Figure 4C, the NY labeling density between 4 and 5 mm from the V1/V2 border is relatively high at that location, whereas the NY labeling near the V1/V2 border represents a very small percentage of the maximum labeling density at that location.

Results from another animal (case mn-18) that received tracer injections in V2 away from the V1/V2 border are shown in Figure 5. In this case, two closely spaced injections of NY were placed approximately 2.0 mm away from the V1/V2 border. A portion of the lateral NY injection, indicated by the box in Figure 5A, is shown in Figure 6A. No NY-labeled cells were found in the ipsilateral LGN. In ipsilateral V1, a single field of NY-labeled cells extended as far as 4.5 mm from the V1 border (see black dots Fig. 5A). It could not be ascertained whether there were NY-labeled cells closer to the V1 border due to the intensity of the fluorescent halo from another V2 tracer injection that was discarded because it invaded the white matter. This labeling pattern in ipsilateral V1 confirms that the NY uptake zone included V2 regions located away from the V1/V2 border (Zeki, 1969; Rockland and Pandya, 1979; Weller and Kaas, 1983; Perkel et al., 1986; Stepniewska and Kaas, 1996; Gattass et al., 1997).

In contralateral V2, few NY-labeled cells were found on or near the V1/V2 border. In contrast, further into V2, NY-labeled cells (Fig. 6B) increased in number and aggregated mainly into three finger-like clusters that were in register with thick CO-dense stripes (Fig. 6C). A few NY-labeled cells were located between these clusters, in register with thin CO-dense stripe (indicated by black arrows in Fig. 6C). These observations are in agreement with Olavarria and Abel (1996). The distribution of NY-labeled callosal cells across V2 (Fig. 5B) differs from the overall pattern of callosal cells in V2 in that, in the latter, the density of callosal cells peaks near the V1/V2 border (cf. Fig. 2A). The normalized distribution of NY-labeled cells across the width of V2 (Fig. 5C) shows that the density of labeled cells approaches the maximum between 2.0 and 2.5 mm from the V1/V2 border, and decreases to significantly lower levels at locations both closer and farther away from the V1/V2 border.

Results from V2 tracer injections located even closer to the V1/V2 border are illustrated in Figure 7. In this animal (case mf-16), two NY-injections, separated by 5.0 mm from each other, were placed close to the lip of the dorsal operculum. The centers of these injections were located approximately 0.7 mm from the V1/V2 border (Fig. 7A). Retrogradely labeled cells in V1 could not be analyzed because the fluorescent halos from the injections extended into regions of V1 where labeled cells would have been expected (Zeki, 1969; Rockland and Pandya, 1979; Weller and Kaas, 1983; Perkel et al., 1986; Stepniewska and Kaas, 1996; Gattass et al., 1997). Sections through the LGN were carefully examined and only a few NY-labeled cells were found near the medial aspect of the nucleus, where the vertical meridian of the visual field (VM) is represented (Malpeli and Baker, 1978; Connolly and Van Essen, 1984). Contralaterally, no NY-labeled cells were found in V1.

In contralateral V2, NY-labeled callosal cells accumulated slightly anterior to the V1/V2 border, closely matching the location of the contralateral NY injections and adjacent regions of intense fluorescent labeling. The density of labeled cells fell sharply at approximately 1.5 mm from the V1/V2 border and labeled cells were virtually absent beyond 2 mm (Fig. 7B). The normalized distribution of NY-labeled cells across the width of V2 (Fig. 7C) indicates that the density of labeled cells approaches the maximum at approximately 0.8 mm from the V1/V2 border and decreases to negligible levels at locations both closer and farther away from the V1/V2 border.

The data described above and presented in Figures 4–7 were obtained from tangential sections of the unfolded and flattened cortex, an approach that permits a detailed analysis of the tangential distribution of injection sites and resulting labeled fields. Similar results were obtained in two additional animals (cases mf-13 and mf-19) whose brains were sectioned in the parasagittal plane, and the results from one of these (case mf-13) are illustrated in Figure 8. In this animal, separate injections of NY were made in medial and lateral portions of dorsal V2 (Fig. 8A). The lateral injection (bottom of Fig. 8A) was located approximately 1.0 mm from the V1/V2 border, whereas the medial injection of NY was placed approximately 2.3 mm from the V1/V2 border. The two NY injections were separated by 3.6 mm from each other. Data on the location of the tracer injections in this case are also shown in Figure 1. The gray region in Figure 1A indicates the portion of the prelunate gyrus that was aspirated to place the injections into V2 of this animal, whereas Figure 1B shows a Nissl-stained parasagittal section passing through the medial NY injection. This section was taken at the location indicated by the black line in Figure 1A. The tangential distribution of NY-labeled callosal cells was reconstructed from a series of parasagittal sections (Fig. 8B). This reconstruction illustrates that the injection closest to the V1/V2 border produced a labeled field that was largely restricted to a strip of cortex occupying the most posterior 2 mm of contralateral V2. In contrast, the labeled field

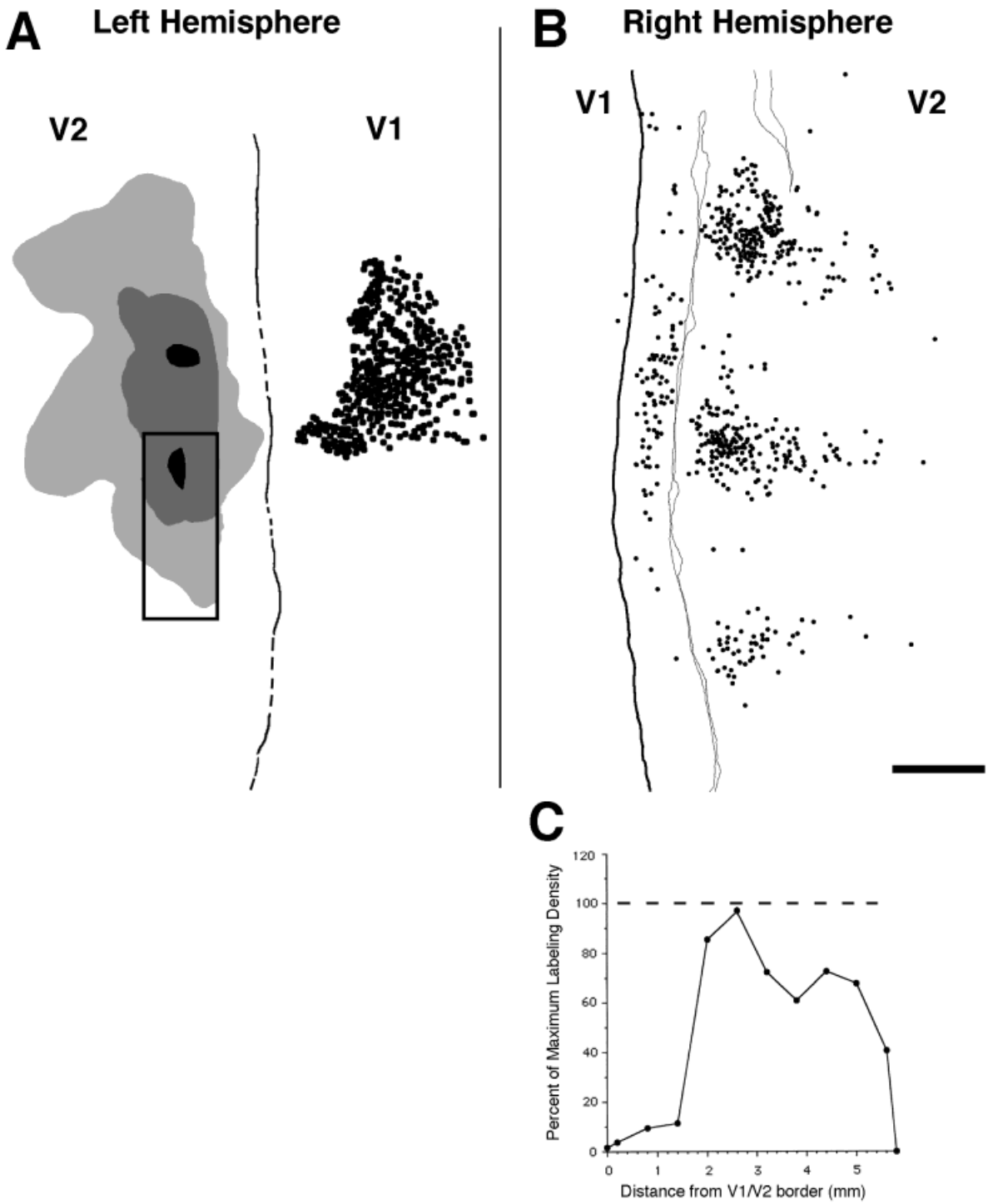

Fig. 5. **A:** Reconstruction of Nuclear Yellow (NY) injection sites in dorsal V2 and of retrogradely labeled fields in ipsilateral V1 (black dots) from tangential sections through the left hemisphere of animal mn-18. Medial is up. At the injection sites, black areas represent the injection cores, whereas the stippled surrounds represent areas of tracer diffusion. The box indicates the region illustrated in Figure 6A. **B:** Distribution of NY-labeled callosal cells (black dots, see Fig. 6B) in dorsal V2 reconstructed from tangential sections through the right hemisphere. Thin lines outline tears in the tissue (cf. Fig. 6C). In A and B, the location of the line indicating the V1/V2 border was determined in cytochrome oxidase-stained sections (see Fig. 6C). Segmented portions of this line in A indicate regions where this border was less clear. **C:** Normalized distribution of NY-labeled callosal cells across the width of V2. Scale bar = 1.5 mm in B (applies to A,B).

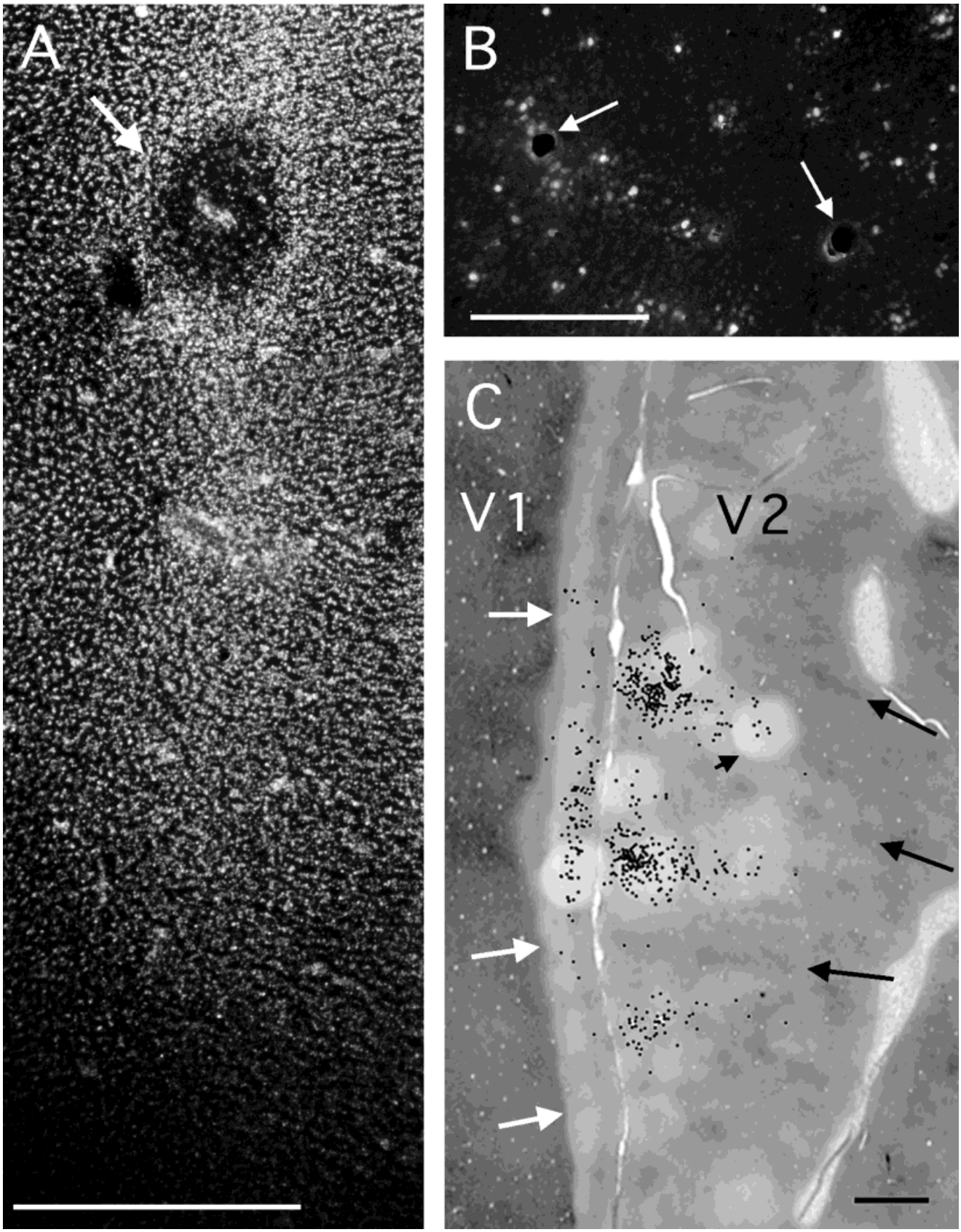

Fig. 6. **A:** Photomontage from a single section showing the injection of Nuclear Yellow (NY) into V2 in monkey mn-18. Image corresponds to area within the box in Figure 5A, and it includes the injection site core (white arrow) and an area of tracer diffusion. **B:** NY-labeled callosal cells from section used to reconstruct the pattern in Figure 5B (also shown in Fig. 6C). Arrows point to blood vessels. Densely NY-labeled nuclei appear as bright dots in A and B. **C:** Digitized image of single tangential cytochrome oxidase (CO) -stained section from the right hemisphere of monkey mn-18 showing the border of V1 (white arrows) and thin CO-dense stripes in V2 (black arrows). The pattern of NY-labeled cells shown in Figure 5B has been superimposed to demonstrate its relationship to the V1/V2 border and CO stripes. This section was stained for CO after being analyzed for fluorescent labeling, which reduced the density of CO staining in areas examined for a long time (e.g., area indicated by short black arrow). Scale bars = 500 μm in A; 125 μm in B; 1.5 mm in C.

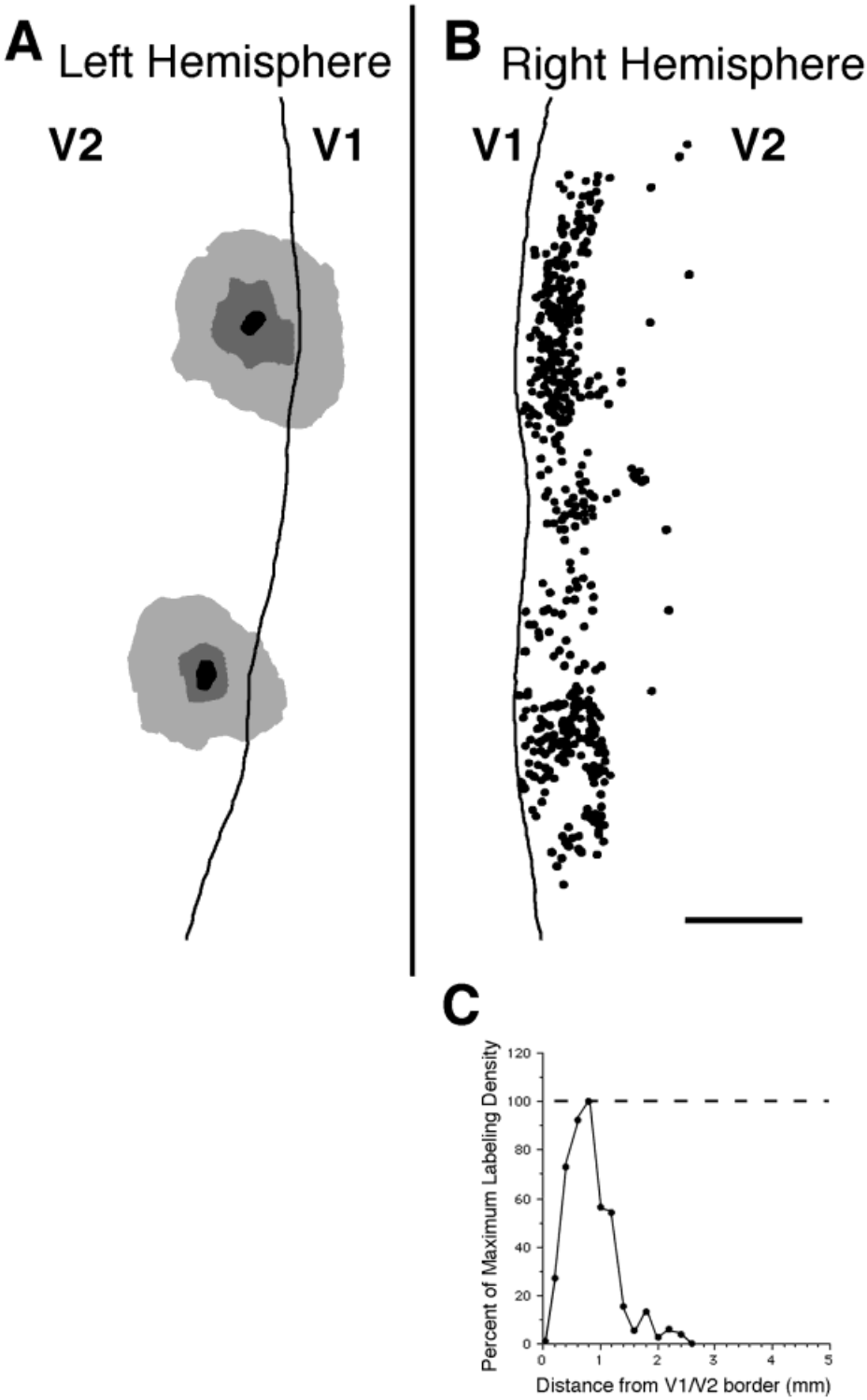

Fig. 7. **A:** Reconstruction of two Nuclear Yellow (NY) injection sites in dorsal V2 from tangential sections through the left hemisphere of animal mf-16. Medial is up. Black areas represent the injection cores, whereas the stippled surrounds represent areas of tracer diffusion. **B:** Distribution of NY-labeled callosal cells (black dots) in dorsal V2 reconstructed from tangential sections through the right hemisphere. In A and B, the location of the line indicating the V1/V2 border was determined in cytochrome oxidase-stained sections. **C:** Normalized distribution of NY-labeled callosal cells across the width of V2. Scale bar = 2.0 mm in B (applies to A,B).

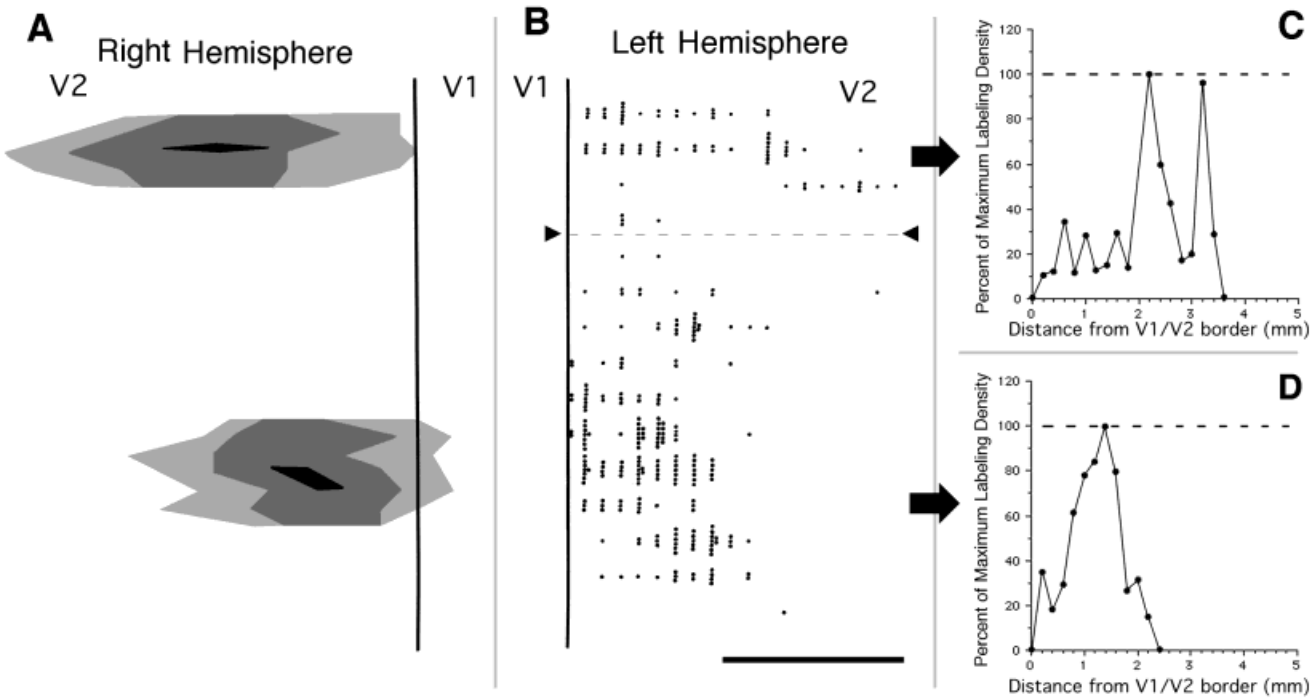

Fig. 8. Distribution of labeled callosal cells in V2 in animal mf-13 analyzed in parasagittal sections. **A:** Reconstruction of two Nuclear Yellow injection sites; black areas represent the injection cores, whereas the stippled surrounds represent areas of tracer diffusion. Medial is up. A dorsal view of the injected hemisphere is shown in Figure 1A, and a Nissl-stained parasagittal section through the medial injection is shown in Figure 1B. **B:** Reconstruction of fields of labeled callosal cells (black dots) in contralateral V2. Labeled cells above the black triangles were considered as being labeled by the top (medial) injection, whereas those below these triangles were considered as being labeled by the bottom (lateral) injection. The location of these triangles corresponds approximately to the lowest density observed between the medial and lateral distributions of labeled cells, and small changes in the location of these triangles do not change the results. In A and B, the V1/V2 border (see Fig. 1B) is represented by black vertical lines. **C,D:** Normalized representations of the corresponding labeled cell distributions shown in B. Scale bar = 2.0 mm in B (applies to A,B).

resulting from the medial injection extended approximately 3.5 mm into contralateral V2. Figure 8C,D indicates that, for each injection, the normalized cell distribution peaks at locations roughly corresponding to the location of the respective injections sites.

DISCUSSION

The results show that varying the distance of V2 tracer injections from the V1/V2 border led to a corresponding variation in the location of labeled callosal cells in contralateral V2. Injections into V2 placed on or close to the V1 border produced labeled cells that accumulated on or close to the V1 border in contralateral V2, whereas injections into V2 placed away from the V1 border produced labeled cells that accumulated preferentially away from the V1 border. These results provide evidence that callosal fibers in V2 preferentially link regions located at similar distances from the V1/V2 border. These findings confirm and extend the results from previous anatomic studies. Myers (1961, 1965) reported that small lesions made within "juxtastriate" cortex produce degeneration in homologous regions in the opposite hemisphere. Subsequent studies in V2 using either the degeneration (Zeki, 1969; Tigges et al., 1974) or the horseradish peroxidase (Tigges et al., 1981; Spatz and Kunz, 1984) techniques reported similar observations. However, these previous studies do not provide information about the organization of callosal linkages throughout the width of the callosal region in V2, because the data presented derive mainly from V2 injections or lesions placed near the V1/V2 border. Cusick and Kaas (1986, 1988) reported that multiple tracer injections largely restricted within area 18 of squirrel monkeys produced callosal labeling in corresponding regions of contralateral area 18, as well as in more posterior regions that included the 17/18 border. There is some evidence from the macaque monkey and other species that callosal connections in other extrastriate visual areas interlink regions that are located at similar distances from the vertical meridian representation (macaques: Van Essen et al., 1982; Maunsell and Van Essen, 1983; cat: Segraves and Rosenquist, 1982a,b; marmosets: Spatz and Tigges, 1972; owl monkeys: Wagor et al., 1975).

Technical considerations

We consistently observed that injections in V2 placed close to the V1/V2 border produced more labeled callosal cells than injections of comparable sizes placed farther away from the V1/V2 border. This decrement in labeling density with distance from the V1/V2 border is less likely to be due to variability in tracer uptake than to the exponential decay of callosal cell density that is observed when the overall pattern of callosal connections in V2 is demonstrated (Fig. 3). To eliminate this confounding factor in

our analysis of the topography of callosal linkages with restricted injections, we expressed the labeling observed at each distance from the V1/V2 border as a percentage of the labeling obtained at the same distance after large tracer injections. These large tracer injections were assumed to reveal the profiles of maximum labeling density across the width of V2 that can be obtained with these methods (Fig. 3). This transformation was not performed in our previous studies of callosal linkages in striate cortex of rats and cats (Lewis and Olavarria, 1995; Olavarria, 1996), which raises the possibility that the different topography of callosal linkages that we report here for macaque V2 is due in part to differences in data analysis. This possibility is unlikely because we confirmed (Olavarria and Abel, unpublished observations) that using this transformation in data from cats does not change the findings presented by Olavarria (1996), namely, injections at the 17/18 border produce callosal labeling in regions located away from the border, whereas injections placed away from the 17/18 border produce callosal labeling at the 17/18 border. For this analysis in the cat, data on the overall distribution of callosal connections were obtained from Bourdet et al. (1996), and data from restricted tracer injections placed at different distances from the 17/18 border were obtained from Olavarria (1996).

To place injections away from the V1/V2 border under visual guidance, we exposed the posterior bank of the lunate sulcus by aspirating portions of the prelunate gyrus. In this condition, it is possible that some of the tracer injected into V2 could have spilled over the exposed white matter in the region of the lesion. Because V2 in the macaque is known to send callosal projections to area V4 located in the prelunate gyrus (Kennedy et al., 1986), the possibility exists that uptake of the tracer by damaged fibers could have led to contralateral labeling in V2. Although we cannot completely rule out this possibility, we believe that uptake from damaged fibers was not significant, because tracer injections placed into the posterior bank of the lunate sulcus consistently produced discrete labeled fields in similar regions of contralateral V2, rather than diffuse labeled fields. Moreover, in a separate group of experiments we placed injections into the intact prelunate gyrus and failed to observe the patterns of contralateral V2 labeling that we obtained after V2 injections (Abel et al., unpublished observations).

Pattern of callosal linkages and visual topography in V2

A recent study of the global pattern of callosal connections in V2 reported that callosal cells accumulate in finger-like bands that protrude 7–8 mm into V2 (Olavarria and Abel, 1996). This distance corresponds to approximately half of the width of V2, which has been estimated to be 10–13 mm (Weller and Kaas, 1983; Van Essen et al., 1990; Olavarria and Van Essen, 1997). Relating the global pattern of callosal connections in V2 with the topographic map of this area (Van Essen and Zeki, 1978; Gattass et al., 1981; Roe and T'so, 1995) suggests that callosal connections can potentially mediate influences from regions representing fields located away from the vertical meridian. An estimate of the extent of the visual field represented in the callosally connected region of V2 can be obtained by correlating the callosal pattern in V2 with previous mapping data from macaque and *Cebus* monkeys, species in which area V2 is similar in both shape and visual topography (Gattass et al., 1981; Van Essen et al., 1986; Rosa et al., 1988). Figure 9 compares schematic representations of the global distribution of callosal connections in V2 (Olavarria and Abel, 1996; present study) with the visual map of this area (Gattass et al., 1981; Van Essen et al., 1986; Rosa et al., 1988). In the visual map, the VM, represented on the V1/V2 border, and the horizontal meridian of the visual field (HM), represented on the anterior border of V2, correspond to the 0-degree and 90-degree isopolar lines, respectively. Moreover, the 45-degree isopolar line for both the lower visual field (represented in dorsal V2) and the upper visual field (represented in ventral V2) corresponds approximately to a line running down the middle of area V2, through points roughly equidistant from the posterior and anterior borders of V2 (see Fig. 9). Figure 9 suggests that the callosally connected region of V2 represents portions of the visual field that can extend from the VM up to the 45-degree isopolar lines (Fig. 9). The present findings suggest that callosal connections near the V1/V2 border interconnect areas representing fields on or close to the VM, whereas callosal connections from regions away from the V1/V2 border interlink visuotopically mismatched fields extending beyond the VM on both hemifields.

Ipsilateral visual field representation in V2

Cells representing ipsilateral visual fields have been reported within macaque V2 (Van Essen and Zeki, 1978; Gattass et al., 1981). In the baboon, Kennedy et al. (1985) reported that some V2 neurons that had ipsilateral visual fields were located as far as 6.0 mm from the V1/V2 border. Ipsilateral visual field representation at the V1/V2 border can be mediated by the nasotemporal overlap at the retinal vertical meridian, i.e., the strip of retina at each side of the vertical meridian where there are both ipsilaterally and contralaterally projecting ganglion cells (Stone et al., 1973; Bunt et al., 1977; Malpeli and Baker, 1978; Leventhal et al., 1988; Fukuda et al., 1989; Chalupa and Lia, 1991). However, the ipsilateral field mediated by this subcortical pathway can be at most approximately 1 degree due of the small size of this overlap in macaque retina. The pattern of callosal linkages that we found in V2 can potentially mediate influences from broader portions of the ipsilateral visual field. Excitatory callosal influences may contribute to the assembly of large bilateral receptive fields whose ipsilateral component depends on the callosal pathway, as is the case for neurons in inferotemporal cortex (Rocha-Miranda et al., 1975). However, because cells with unusually large receptive fields have not been reported in previous physiologic studies of macaque V2 (Van Essen and Zeki, 1978; Gattass et al., 1981; Roe and Ts'o, 1995), excitatory callosal influences may contribute to modulatory surrounds beyond the classic receptive fields. Likewise, inhibitory callosal influences could potentially contribute to large silent surrounds extending into the ipsilateral field and exerting suppressive modulation of classic receptive fields close to the midline, as occurs in V4 (Desimone et al., 1993) and MT (Allman et al., 1985). Motter and Mountcastle (1981) reported that many light-sensitive cells in the posterior parietal cortex of monkeys responded to stimuli within disjointed areas of the visual field located on either side of the fixation point, and it will be interesting to study whether interhemispheric connections play a role in the assembly of these bilateral receptive fields.

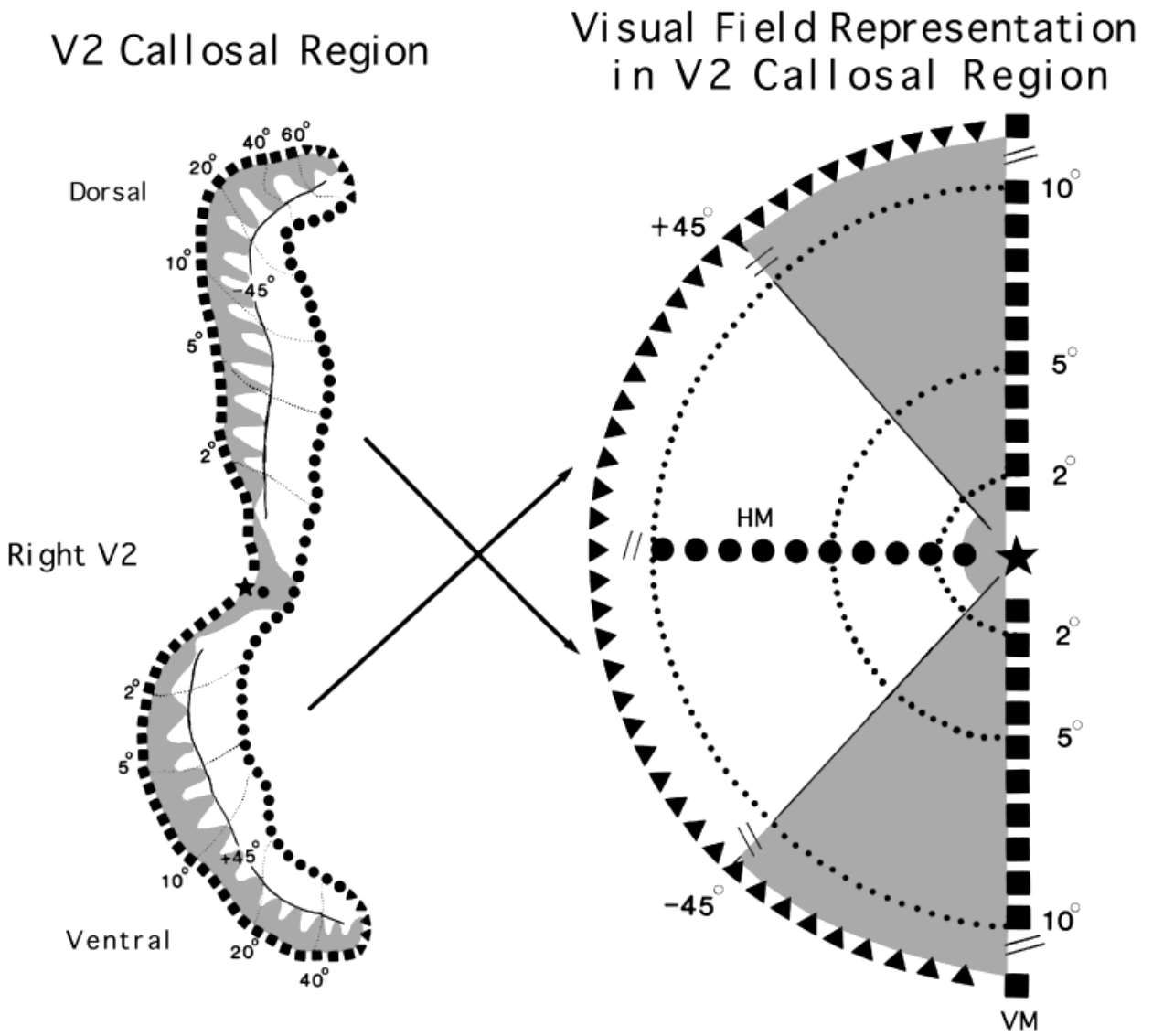

Fig. 9. Correlating the callosal pattern and the visual field map in area V2. The left panel shows a schematic representation of the overall pattern of callosal connections (in gray) in dorsal and ventral halves of right area V2 superimposed to mapping data from V2 (Gattass et al., 1981; Van Essen et al., 1986; Rosa et al., 1988). Posterior is to the left. The symbols in the topographic map correspond with those in the left visual hemifield represented in the right panel. The arrows between left and right panels indicate that dorsal and ventral V2 represent lower and upper visual field quadrants, respectively. The posterior border of V2 represents the vertical meridian (black squares), the anterior border represents the horizontal meridian (large dots), the uppermost and lowermost regions of V2 represent peripheral fields (triangles), and the foveal representation is in the middle of V2 (star). Isoeccentricity lines are represented with small dots and isopolar lines with thin lines. The shaded area in the hemifield corresponds approximately to the extent of the visual field represented in the callosally connected region in V2.

Callosal connections in V2 correlate with CO-dense thick and thin stripes (Olavarria and Abel, 1996), opening the possibility that callosal input influences the mapping of visual fields in these stripes. Although this issue has not been directly investigated, the available mapping data in V2 do not support the idea that receptive fields in CO-dense stripes preferentially include the VM or extend into the ipsilateral field (Hubel and Livingstone, 1987; Peterhans and von der Heydt, 1993, Levitt et al., 1994; Munk et al., 1995; Roe and Ts'o, 1995; Gegenfurtner et al., 1996; Yoshioka and Dow, 1996). However, a recent study of the visual field representations within the different CO compartments in V2 found some differences in the amount of receptive field scatter, receptive field size, or cortical magnification factor between the different V2 compartments (Roe and Ts'o, 1995). Whether or not callosal connections contribute to these differences remains to be investigated.

Callosal connections and midline stereopsis

Depth perception for objects located in the midline of the visual field (midline stereopsis) poses a problem, because the retinal images for objects that are either in front or

behind the fixation point fall upon nasal or temporal retina in *both* eyes (see Blakemore, 1969, and references therein). For sufficiently small disparities, within the range required for "fine" stereopsis (Bishop and Henry, 1971), these images would fall in the region of retinal nasotemporal overlap, being, thus, relayed to the same hemisphere for cortical binocular processing. However, there is evidence that midline depth discrimination of a coarser kind (referred to as "coarse" stereopsis by Bishop and Henry, 1971) can be made with disparities up to 7–10 degrees which are significantly larger than the nasotemporal overlap in macaque monkeys and humans (Westheimer and Tanzman, 1956). In this case, the images in each eye of objects either in front or behind the fixation point fall outside the region of nasotemporal overlap, being therefore relayed to different hemispheres (see Fig. 10 in Blakemore, 1969). How do these disparate images come together for binocular processing? Studies on a patient that had undergone surgical section of the corpus callosum suggests that, in humans, the mechanisms for midline coarse stereopsis (Mitchell and Blakemore, 1970) and for initiating vergence eye movements (Westheimer and Mitchell, 1969), require intact interhemispheric connections.

Callosal connections in macaque V1 are not well suited for mediating coarse stereopsis at the midline, because they are restricted to a narrow region representing approximately 1 degree of visual field. In contrast, callosally connected regions in V2 (see above) and other extrastriate areas (e.g., Van Essen et al., 1982; Maunsell and Van Essen, 1983) represent a wider portion of the visual field, therefore, being better suited for mediating midline coarse stereopsis and initiation of vergence eye movements. Similar considerations may apply to humans, because the distribution of callosal connections in human visual cortex resembles that in macaques (Clarke and Miklossy, 1990; Van Essen et al., 1995). For disparities in the range of coarse stereopsis, binocular processing of stimuli placed either in front or behind the fixation point would seem to require the existence of interhemispheric links between cortical regions the represent visual fields arranged symmetrically on both sides of the vertical meridian (see Fig. 10 in Blakemore, 1969). The results of the present study make area V2 a good candidate for mediating coarse midline stereopsis and initiation of vergence eye movements. Other extrastriate visual areas may also play a role in these functions. For instance, callosal connections in MT (Spatz and Tigges, 1972; Maunsell and Van Essen, 1983; Weller et al., 1984) and in cat suprasylvian cortex (Segraves and Rosenquist, 1982a,b) appear to interlink loci representing paracentral receptive visual fields.

Specification of callosal linkages in V1 and V2

Comparison of our present results with previous studies in V1 suggests a striking difference between the organization of callosal linkages in striate and extrastriate cortex. The present study shows that callosal connections in V2 interconnect loci that are located at similar distances from the V1/V2 border, whereas in V1 of rats and cats callosal fibers link loci that are in retinotopic, rather than anatomic, correspondence (Lewis and Olavarria, 1995; Olavarria, 1996). Based on information that each temporal retina projects bilaterally in rats (Lund et al., 1974) and cats (Fukuda and Stone, 1974), Olavarria and Li (1995) proposed that the development of retinotopically corresponding linkages in V1 depends on correlations in interhemispheric activity that are derived from correlations in the activity of neighboring ganglion cells located in the temporal retina of each eye. In support of this hypothesis, Olavarria and Li (1995) showed that retinal activity is necessary for the development of retinotopically corresponding callosal linkages in V1. Although prenatal removal of retinal input alters the pattern of callosal connections in macaque V2 (Dehay et al., 1989), it seems unlikely that retinal activity cues guide the stabilization of topographically mirror-symmetric callosal linkages in this visual area. The stabilization of callosal linkages in V2 may depend instead on chemical or other positional cues (Olavarria and Li, 1995). It is possible that the role the eyes play in the development of callosal connections differs in striate and extrastriate cortex, even in the same species. Support for this idea comes from the observation in cats that neonatal elimination of retinal activity or visual experience has pronounced effects on the distribution and density of callosal cells at the V1 border, with little or no effect in extrastriate cortex (Olavarria, 1995; Olavarria and Van Sluyters, 1995). Understanding the cellular bases for this difference may yield valuable clues for identifying the mechanisms that guide the development and organization of corticocortical pathways in striate and extrastriate visual areas.

ACKNOWLEDGMENTS

We thank August Zitzka for helping with laboratory procedures.

LITERATURE CITED

Abel PL, O'Brien BJ, Olavarria JF. 1995. Callosal connections interlink anatomically corresponding regions in visual area V2 of macaque monkey. Soc Neurosci Abstr 21:903.

Abel PL, O'Brien BJ, Lia B, Olavarria JF. 1997. Distribution of neurons projecting to the superior colliculus correlates with thick cytochrome oxidase stripes in macaque visual area V2. J Comp Neurol 377:313–323.

Allman J, Miezin F, McGuinness E. 1985. Stimulus specific responses from beyond the classical receptive field: neurophysiological mechanisms for local-global comparisons in visual neurons. Annu Rev Neurosci 8:407–430.

Bishop PO, Henry GH. 1971. Spatial vision. Annu Rev Psychol 22:119–161.

Blakemore C. 1969. Binocular depth discrimination and the nasotemporal division. J Physiol 205:471–497.

Bourdet C, Olavarria JF, Van Sluyters RC. 1996. Distribution of visual callosal neurons in normal and strabismic cats. J Comp Neurol 366: 259–269.

Bunt AH, Minkler DS, Johanson GW. 1977. Demonstration of bilateral projection of the central retina of the monkey with horseradish peroxidase neuronography. J Comp Neurol 171:619–630.

Chalupa LM, Lia B. 1991. The nasotemporal division of retinal ganglion cells with crossed and uncrossed projections in the fetal rhesus monkey. J Neurosci 11:191–202.

Clarke S, Miklossy J. 1990. Occipital cortex in man: organization of callosal connections, related myelo- and cytoarchitecture, and putative boundaries of functional visual areas. J Comp Neurol 298:188–214.

Connolly M, Van Essen DC. 1984. The representation of the visual field in parvicellular and magnocellular layers of the lateral geniculate nucleus in the macaque monkey. J Comp Neurol 226:544–564.

Cragg BG. 1969. The topography of afferent projections in the circumstriate visual cortex of the monkey studied by the Nauta method. Vision Res 9:733–747.

Cusick CG, Kaas JH. 1986. Interhemispheric connections of cortical sen-

sory and motor representations in primates. In: Lepore F, Ptito M, Jasper HH, editors. Two hemispheres-one brain: functions of the corpus callosum. New York: Alan R. Liss. p 83–102.

Cusick CG, Kaas JH. 1988. Cortical connections of area 18 and dorsolateral visual cortex in squirrel monkeys. Vis Neurosci 1:211–237.

Cusick CG, Gould HJ III, Kaas JH. 1984. Interhemispheric connections of visual cortex of owl monkeys (*Aotus trivirgatus*), marmosets (*Callithrix jacchus*), and galagos (*Galago crassicaudatus*). J Comp Neurol 230: 311–336.

Cusick CG, MacAvoy MG, Kaas JH. 1985. Interhemispheric connections of cortical sensory areas in tree shrews. J Comp Neurol 235:111–128.

Dehay C, Horsburgh G, Berland M, Killackey H, Kennedy H. 1989. Maturation and connectivity of the visual cortex in monkey is altered by prenatal removal of retinal input. Nature 337:265–267.

Desimone R, Moran J, Schein SJ, Mishkin M. 1993. A role for the corpus callosum in visual area V4 of the macaque. Vis Neurosci 10:159–171.

DeYoe EA, Hockfield S, Garren H, Van Essen DC. 1990. Antibody labeling of functional subdivisions in visual cortex: Cat-301 immunoreactivity in striate and extrastriate cortex of macaque monkey. Vis Neurosci 5:67–81.

Ebner FF, Myers RE. 1965. Distribution of corpus callosum and anterior commissure in the cat and the raccoon. J Comp Neurol 124:353–365.

Fukuda Y, Stone J. 1974. Retinal distribution and central projections of Y, X, and W cells in the cat's retina. J Neurophysiol 37:749–772.

Fukuda Y, Sawai H, Watanabe M, Wakakuwa K, Morigiwa K. 1989. Nasotemporal overlap of crossed and uncrossed retinal ganglion cell projections in the Japanese monkey (*Macaca fuscata*). J Neurosci 9:2353–2373.

Gattass R, Gross CG, Sandell JH. 1981. Visual topography of V2 in the macaque. J Comp Neurol 201:519–539.

Gattass R, Sousa APB, Mishkin M, Ungerleider LG. 1997. Cortical projections of area V2 in the macaque. Cereb Cortex 7:110–129.

Gegenfurtner KR, Kiper DC, Fenstemaker SB. 1996. Processing of color, form and motion in macaque area V2. Vis Neurosci 13:161–172.

Hendry SHC, Jones EG, Hockfield S, McKay RDG. 1988. Neuronal populations stained with the monoclonal antibody Cat-301 in the mammalian cerebral cortex and thalamus. J Neurosci 8:518–542.

Hubel DH, Livingstone MS. 1987. Segregation of form, color and stereopsis in primate area 18. J Neurosci 7:3378–3415.

Hubel DH, Wiesel TN. 1967. Cortical and callosal connections concerned with the vertical meridian of visual fields in the cat. J Neurophysiol 30:1561–1573.

Kennedy H, Martin KAC, Orban GA, Whitteridge D. 1985. Receptive field properties of neurons in visual area I and visual area II in the baboon. Neuroscience 14:405–415.

Kennedy H, Dehay C, Bullier J. 1986. Organization of the callosal connections of visual areas V1 and V2 in the macaque monkey. J Comp Neurol 247:398–415.

Leventhal AG, Ault SJ, Vitek DJ. 1988. The nasotemporal division in primate retina: the neural basis of macular sparing and splitting. Science 240:66–67.

Levitt JB, Kiper DC, Movshon JA. 1994. Receptive fields and functional architecture of macaque V2. J Neurophysiol 71:2517–2542.

Lewis JW, Olavarria JF. 1995. Two rules for callosal connectivity in striate cortex of the rat. J Comp Neurol 361:119–137.

Lund JS, Lund RD, Hendrickson AE, Bunt AH, Fuchs AF. 1975. The origin of efferent pathways from primary visual cortex, area 17, of the macaque monkey as shown by retrograde transport of horseradish peroxidase. J Comp Neurol 164:287–304.

Lund RD, Lund JS, Wise RP. 1974. The organization of the retinal projection to the dorsal lateral geniculate nucleus in pigmented and albino rats. J Comp Neurol 158:383–404.

Malpeli JG, Baker FH. 1978. The representation of the visual field in the lateral geniculate nucleus of *Macaca mulatta*. J Comp Neuol 161:569–594.

Maunsell JHR, Van Essen DC. 1983. The connections of the middle temporal visual area (MT) and their relationship to a cortical hierarchy in the macaque monkey. J Neurosci 3:2563–2586.

Maunsell JHR, Van Essen DC. 1987. Topographic organization of the middle temporal visual area in the macaque monkey: representational biases and the relationship to callosal connections and myeloarchitectonic boundaries. J Comp Neurol 266:535–555.

Mettler FA. 1935. Coticofugal fiber connections of the cortex of *Macaca mullatta*: the occipital region. J Comp Neurol 61:221–256.

Mitchell DE, Blakemore C. 1970. Binocular depth perception and the corpus callosum. Vision Res 10:49–54.

Motter BC, Mountcastle VB. 1981. The functional properties of the light-sensitive neurons of the posterior parietal cortex studied in waking monkeys: foveal sparing and opponent vector organization. J Neurosci 1:3–26.

Munk MHJ, Nowak LG, Girard P, Chounlamountri N, Bullier J. 1995. Visual latencies in cytochrome oxidase bands of macaque area V2. Proc Natl Acad Sci USA 92:988–992.

Myers RE. 1961. Contralateral projections of juxta-striate parts of cortical area 18 in the monkey. Anat Rec 139:259.

Myers RE. 1962. Commissural connections between occipital lobes of the monkey. J Comp Neurol 118:1–16.

Myers RE. 1965. The neocortical commissures and interhemispheric transmission of information. In: Ettlinger EG, editor. Functions of corpus callosum. Boston: Brown & Co. p 1–17.

Olavarria JF. 1995. The effect of visual deprivation on the number of callosal cells in the cat is less pronounced in extrastriate cortex than in the 17/18 border region. Neurosci Lett 195:147–150.

Olavarria JF. 1996. Non mirror symmetric pattern of callosal linkages in areas 17 and 18 in cat visual cortex. J Comp Neurol 366:643–655.

Olavarria JF, Abel PL. 1996. The distribution of callosal connections correlates with the pattern of cytochrome oxidase stripes in visual area V2 of macaque monkeys. Cereb Cortex 6:631–639.

Olavarria JF, Li Ch-P. 1995. Effects of neonatal enucleation on the organization of callosal linkages in striate cortex of the rat. J Comp Neurol 361:138–151.

Olavarria JF, Van Essen DC. 1997. The global pattern of cytochrome oxidase stripes in visual area V2 of the macaque monkey. Cereb Cortex 7:395–404.

Olavarria J, Van Sluyters RC. 1983. Widespread callosal connections in infragranular visual cortex of the rat. Brain Res 279:233–237.

Olavarria J, Van Sluyters RC. 1985. Unfolding and flattening the cortex of gyrencephalic brains. J Neurosci Methods 15:191–202.

Olavarria JF, Van Sluyters RC. 1995. The overall pattern of callosal connections in visual cortex of normal and enucleated cats. J Comp Neurol 363:161–173.

Perkel DJ, Bullier J, Kennedy H. 1986. Topography of afferent connectivity of area 17 in the macaque monkey: a double-labelling study. J Comp Neurol 253:374–402.

Peterhans E, von der Heydt R. 1993. Functional organization of area V2 in the alert macaque. Eur J Neurosci 5:509–524.

Rocha-Miranda CE, Bender DB, Gross CG, Mishkin M. 1975. Visual activation of neurons in inferotemporal cortex depends on striate cortex and forebrain commissures. J Neurophysiol 38:475–491.

Rockland KS, Pandya DN. 1979. Laminar origins and terminations of cortical connections of the occipital lobe in the rhesus monkey. Brain Res 179:3–20.

Roe AW, Ts'o DY. 1995. Visual topography in primate V2: multiple representations across functional stripes. J Neurosci 15:3689–3715.

Rosa MGP, Sousa APB, Gattass R. 1988. Representation of the visual field in the second visual area in the *Cebus* monkey. J Comp Neurol 275: 326–345.

Segraves MA, Rosenquist AC. 1982a. The distribution of the cells of origin of callosal projections in cat visual cortex. J Neurosci 2:1079–1089.

Segraves MA, Rosenquist AC. 1982b. The afferent and efferent callosal connections of retinotopically defined areas in cat cortex. J Neurosci 2:1090–1107

Spatz WB, Kunz B. 1984. Area 17 of anthropoid primates does participate in visual callosal connections. Neurosci Lett 48:49–53.

Spatz WB, Tigges J. 1972. Experimental-anatomical studies on the "middle temporal visual areas (MT)" in primates: I. Efferent corticocortical connections in the marmoset *Callithrix jacchus*. J Comp Neurol 146: 451–464.

Stepniewska I, Kaas JH. 1996. Topographic patterns of V2 cortical connections in macaque monkeys. J Comp Neurol 371:129–152.

Stone J, Leicester J, Sherman SM. 1973. The naso-temporal division of the monkey's retina. J Comp Neurol 150:333–348.

Tigges J, Spatz WB, Tigges M. 1974. Efferent cortico-cortical fiber connections of area 18 in the squirrel monkey (*Saimiri*). J Comp Neurol 158:219–236.

Tigges J, Tigges M, Anschel S, Cross NA, Letbetter WD, McBride RL. 1981. Areal and laminar distribution of neurons interconnecting the central

visual cortical areas 17, 18, 19, and MT in squirrel monkey (*Saimiri*). J Comp Neurol 202:539–560.

Van Essen DC, Zeki SM. 1978. The topographic organization of rhesus monkey prestriate cortex. J Physiol (Lond) 277:193–226.

Van Essen DC, Newsome WT, Bixby JL. 1982. The pattern of interhemispheric connections and its relationship to extrastriate visual areas in the macaque monkey. J Neurosci 2:265–283.

Van Essen DC, Newsome WT, Maunsell JHR, Bixby JL. 1986. The projections from striate cortex (V1) to areas V2 and V3 in the macaque monkey: asymmetries, areal boundaries, and patchy connections. J Comp Neurol 244:451–480.

Van Essen DC, Felleman DJ, DeYoe EA, Olavarria J, Knierim J. 1990. Modular and hierarchical organization of extrastriate visual cortex in the macaque monkey. Cold Spring Harbor Symp Quant Biol 55:679–695.

Van Essen DC, Clarke S, Drury, Hadjikhani N, Coogan T, Kraftsik R. 1995. Organization of extrastriate visual areas in human occipital cortex inferred from callosal connections. Soc Neurosci Abstr 21:1274.

Wagor E, Lin CS, Kaas JH. 1975. Some cortical projections of the dorsomedial visual area (DM) of association cortex in the owl monkey, *Aotus trivirgatus*. J Comp Neurol 163:227–250.

Weller RE, Kaas JH. 1983. Retinotopic patterns of connections of area 17 with visual areas V-II and MT in macaque monkeys. J Comp Neurol 220:253–279.

Weller RE, Wall JT, Kaas JH. 1984. Cortical connections of the middle temporal visual area (MT) and the superior temporal cortex in owl monkeys. J Comp Neurol 228:81–104.

Westheimer G, Mitchell DE. 1969. The stimulus for convergence and divergence eye movements. Vision Res 9:749–755.

Westheimer G, Tanzman IJ. 1956. Qualitative depth localization with diplopic images. J Opt Soc Am 46:116–117.

Wong-Riley M. 1979. Changes in the visual system of monocularly sutured or enucleated cats demonstrable with cytochrome oxidase histochemistry. Brain Res 171:11–28.

Yoshioka T, Dow BM. 1996. Color, orientation and cytochrome oxidase reactivity in areas V1, V2, and V4 of macaque monkey visual cortex. Behav Brain Res 76:71–88.

Zeki SM. 1969. Representation of central visual fields in prestriate cortex of monkey. Brain Res 14:271–291.

Zeki SM. 1970. Interhemispheric connections of prestriate cortex in monkey. Brain Res 19:63–75.